Nanoscale Res Lett (2010) 5:1546–1554
DOI 10.1007/s11671-010-9675-1

NANO EXPRESS

Dimensional Effects on Densities of States and Interactions in Nanostructures

Rainer Dick

Received: 15 April 2010 / Accepted: 7 June 2010 / Published online: 2 July 2010

Abstract We consider electrons in the presence of interfaces with different effective electron mass, and electromagnetic fields in the presence of a high-permittivity interface in bulk material. The equations of motion for these dimensionally hybrid systems yield analytic expressions for Green's functions and electromagnetic potentials that interpolate between the two-dimensional logarithmic potential at short distance, and the three-dimensional r^{-1} potential at large distance. This also yields results for electron densities of states which interpolate between the well-known two-dimensional and three-dimensional formulas. The transition length scales for interfaces of thickness L are found to be of order $Lm/2m_*$ for an interface in which electrons move with effective mass m_*, and $L\epsilon_*/2\epsilon$ for a dielectric thin film with permittivity ϵ_* in a bulk of permittivity ϵ. We can easily test the merits of the formalism by comparing the calculated electromagnetic potential with the infinite series solutions from image charges. This confirms that the dimensionally hybrid models are excellent approximations for distances $r \gtrsim L/2$.

Keywords Density of states · Coulomb and exchange interactions in nanostructures · Dielectric thin films

R. Dick (✉)
Physics & Engineering Physics, University of Saskatchewan, 116 Science Place, Saskatoon, SK S7N 5E2, Canada
e-mail: rainer.dick@usask.ca

Introduction

When we suppress motion of particles in certain directions through confining potentials, e.g. in quantum wells or quantum wires, we often model the residual low energy excitations in the system through low-dimensional quantum mechanical systems. Prominent examples of this concern layered heterostructures, and one instance where the number d of spatial dimensions enters in a manner which is of direct relevance to technology is in the density of states. In the standard parabolic band approximation, this takes the form (with two helicity or spin states)

$$\varrho_{(d)}(E) = 2\Theta(E)\sqrt{\frac{m}{2\pi}}^{d}\frac{\sqrt{E}^{d-2}}{\Gamma(d/2)\hbar^d}. \tag{1}$$

These are densities of states per d-dimensional volume and per unit of energy. The corresponding dependence of the relation between the Fermi energy and the density n of electrons on d is

$$n_{(d)} = \frac{2}{\hbar^d\Gamma((d+2)/2)}\sqrt{\frac{mE_F}{2\pi}}^{d}. \tag{2}$$

Variants of these equations (including summation over subbands) are often used for $d = 2$ or $d = 1$ to estimate carrier densities in quasi two-dimensional systems or nanowires, and the density of states plays a crucial role in all transport and optical properties of materials. Indeed, the obvious relevance for electrical conductivity properties in micro and nanotechnology implies that densities of states for $d = 1$, 2, or 3 are now commonly discussed in engineering textbooks, but there is another reason why I anticipate that variants of Eq. (1) will become ever more prominent in the technical literature. Densities also play a huge role in data storage, but with us still relying on binary

logic switching between two stable states (spin up or down, charge or no charge, conductivity or no conductivity), data storage densities are limited by the physical densities of the systems which provide the dual states. We could (and likely will) drive information technology and integration much further if we can find ways to utilize more than just two states of a physical system to store and process information. Then, data storage densities should become proportional to energy integrals $\int_{\Delta E} dE \varrho(E)$ of local densities of states. Equation (1) for $d = 1$ or $d = 2$ is certainly applicable for particles which have low energies compared to the confinement energy of a nanowire or a quantum well, but how can we effectively model particles which are weakly confined to a nanowire or quantum well, or which are otherwise affected by the presence of a low-dimensional substructure? In these cases, we can devise dimensionally hybrid models [1, 2] which yield e.g. densities of states which interpolate between $d = 2$ and $d = 3$ [3, 4]. This construction will be reviewed in Sect. 2. Based on the experience gained with dimensionally hybrid Hamiltonians for massive particles, we can also construct inter-dimensional Hamiltonians for photons which should be applicable to photons in the presence of high-permittivity thin films or interfaces. These models can also be solved in terms of infinite series expansions using image charges, and the merits of this approach can easily be tested. The case of high-permittivity thin films and testing the theory against image charge solutions will be discussed in Sect. 3.

Dimensionally Hybrid Hamiltonians and Green's Functions for Massive Particles in the Presence of Thin Films or Interfaces

We use the connection between Green's functions and the density of states to generalize Eq. (1) for massive particles in the presence of a thin film or interface.

The energy-dependent Green's function for a Hamiltonian H with spectrum E_n and eigenstates $|n, \nu\rangle$ is

$$\begin{aligned}\mathcal{G}(E) &= -\frac{2m}{\hbar^2}G(E) = \frac{1}{E - H + \mathrm{i}\epsilon} = \sum \int_{n,\nu} \frac{|n,\nu\rangle\langle n,\nu|}{E - E_n + \mathrm{i}\epsilon} \\ &= \mathcal{P}\sum \int_{n,\nu} \frac{|n,\nu\rangle\langle n,\nu|}{E - E_n} \\ &\quad - \mathrm{i}\pi \sum \int_{n,\nu} \delta(E - E_n)|n,\nu\rangle\langle n,\nu|. \end{aligned} \tag{3}$$

Here, ν is a degeneracy index and the notation implies that continuous components in the indices (n, ν) are integrated. The first equation simply states the relation between the resolvent $\mathcal{G}(E)$ of the Hamiltonian and the Green's function $G(E)$ which is normalized as $\lim_{m\to 0, E\to 0} G(E)|_{d=3} = (4\pi r)^{-1}$.

The zero-energy Green's function $G(0)$ determines e.g. 2-particle correlation functions and electromagnetic interaction potentials, and the energy-dependent Green's function $G(E)$ determines e.g. scattering amplitudes for particles of energy E. Application for resistivity calculations is therefore another technologically relevant application of Green's functions. However, in the present section we are interested in this function because it also determines the local density of states in a system with Hamiltonian H through the relation

$$\varrho(E_n, \vec{x}) = 2\sum \int_{\nu} \langle \vec{x}|n,\nu\rangle\langle n,\nu|\vec{x}\rangle = \frac{4m}{\pi\hbar^2}\Im\langle \vec{x}|G(E_n)|\vec{x}\rangle. \tag{4}$$

Here, we explicitly included a factor 2 for the number of spin or helicity states, because the summation over degeneracy indices in (3,4) usually only involves orbital indices.

For our present investigation, the distinctive feature of the interface is that the particles move in it with an effective mass m_*, while their mass in the surrounding bulk is m. We use coordinates $\boldsymbol{x} = \{x, y\}$ parallel to a plane interface, which is located at $z = z_0$. Bold vector notation is used for quantities parallel to the interface, e.g. $\vec{p} = \{\boldsymbol{p}, p_z\}$ and $\vec{\nabla} = \{\boldsymbol{\nabla}, \partial_z\}$.

We assume that the interface has a thickness L. If the wavenumber component orthogonal to the interface is small compared to the inverse width, $|k_\perp L| \ll 1$, i.e. if the de Broglie wavelength and the incidence angle satisfy $\lambda \gg 2\pi L|\cos\vartheta|$, we can approximate the kinetic energy of the particles through a second quantized Hamiltonian

$$\begin{aligned} H = &\int \mathrm{d}^2\boldsymbol{x} \int \mathrm{d}z \frac{\hbar^2}{2m}\vec{\nabla}\psi^+(\boldsymbol{x}, z)\cdot\vec{\nabla}\psi(\boldsymbol{x}, z) \\ &+ \int \mathrm{d}^2\boldsymbol{x}\frac{\hbar^2}{2\mu}\boldsymbol{\nabla}\psi^+(\boldsymbol{x}, z_0)\cdot\boldsymbol{\nabla}\psi(\boldsymbol{x}, z_0), \end{aligned} \tag{5}$$

where $\mu = m_*/L$. The corresponding first quantized Hamiltonian is

$$H = \frac{\boldsymbol{p}^2 + p_z^2}{2m} + |z_0\rangle\langle z_0|\frac{\boldsymbol{p}^2}{2\mu}. \tag{6}$$

The interesting aspect of the Hamiltonians (5,6) is the linear superposition of two-dimensional and three-dimensional kinetic terms. The formalism presented here could and will certainly be extended to include also kinetic terms which are linear in derivatives, in particular in the interface term. This would be motivated either by a Rashba term arising from perpendicular fields penetrating the interface [5–11] of from the dispersion relation in Graphene [12–15]. However, for the present investigation

we will use a parabolic band approximation in the bulk and in the interface.

The energy-dependent Green's function $\langle\vec{x}|G(E)|\vec{x}'\rangle \equiv \langle z|G(E;\boldsymbol{x}-\boldsymbol{x}')|z'\rangle$ describes scattering effects in the presence of the interface but also applies to scattering off perturbations which are not located on the interface. In an axially symmetric mixed representation

$$\langle \boldsymbol{k}, z|G(E)|\boldsymbol{k}', z'\rangle = \langle z|G(E;\boldsymbol{k})|z'\rangle\delta(\boldsymbol{k}-\boldsymbol{k}') \tag{7}$$

the first order approximation to scattering of an orthogonally incoming plane wave off an impurity potential

$$V(\boldsymbol{x}, z) = \frac{1}{4\pi^2}\int \mathrm{d}^2\boldsymbol{k} V(\boldsymbol{k}, z)\exp(\mathrm{i}\boldsymbol{k}\cdot\boldsymbol{x})$$

corresponds to

$$\begin{aligned}\psi(\boldsymbol{x}, z) =& \frac{1}{\sqrt{2\pi}^3}\Bigg[\exp(\mathrm{i}k_\perp z) - \frac{m}{2\pi^2\hbar^2}\int \mathrm{d}^2\boldsymbol{x}'\int \mathrm{d}^2\boldsymbol{k}\\ &\times\int \mathrm{d}z'\langle z|G(E;\boldsymbol{k})|z'\rangle V(\boldsymbol{x}', z')\\ &\times\exp[\mathrm{i}(\boldsymbol{k}\cdot\boldsymbol{x}+k_\perp z')]\exp(-\mathrm{i}\boldsymbol{k}\cdot\boldsymbol{x}')\Bigg]\\ =& \frac{1}{\sqrt{2\pi}^3}\Bigg[\exp(\mathrm{i}k_\perp z) - \frac{m}{2\pi^2\hbar^2}\int \mathrm{d}^2\boldsymbol{k}\\ &\int \mathrm{d}z'\langle z|G(E;\boldsymbol{k})|z'\rangle V(\boldsymbol{k}, z')\exp[\boldsymbol{i}(\boldsymbol{k}\cdot\boldsymbol{x}+\boldsymbol{k}_\perp z')]\Bigg].\end{aligned}$$

Green's functions for surfaces or interfaces are commonly parametrized in an axially symmetric mixed representation like $G(E;\boldsymbol{k}, z, z')$. In bra-ket notation, this corresponds for the free Green's function $G_0(E)$, which is also translation invariant in z direction, to

$$\langle \boldsymbol{k}, z|G_0(E)|\boldsymbol{k}', z'\rangle = G_0(E;\boldsymbol{k}, z-z')\delta(\boldsymbol{k}-\boldsymbol{k}').$$

We will briefly recall the explicit form of the free Green's function $G_0(E)$ in the axially symmetric mixed parametrization for later comparison. The equation

$$\left(\partial_z^2 - \boldsymbol{k}^2 + \frac{2mE}{\hbar^2}\right)G_0(E;\boldsymbol{k}, z) = -\delta(z)$$

yields

$$\begin{aligned}G_0(E;\boldsymbol{k}, z) =& \frac{1}{2\pi}\int \mathrm{d}k_\perp \frac{\exp(\mathrm{i}k_\perp z)}{k_\perp^2 + \boldsymbol{k}^2 - (2mE/\hbar^2) - \mathrm{i}\epsilon}\\ =& \frac{\hbar\Theta(\hbar^2\boldsymbol{k}^2 - 2mE)}{2\sqrt{\hbar^2\boldsymbol{k}^2 - 2mE}}\exp\left(-\sqrt{\hbar^2\boldsymbol{k}^2 - 2mE}\frac{|z|}{\hbar}\right)\\ &+\frac{\mathrm{i}\hbar\Theta(2mE - \hbar^2\boldsymbol{k}^2)}{2\sqrt{2mE - \hbar^2\boldsymbol{k}^2}}\exp\left(\mathrm{i}\sqrt{2mE - \hbar^2\boldsymbol{k}^2}\frac{|z|}{\hbar}\right).\end{aligned} \tag{8}$$

To study how this is modified in the presence of the interface, we observe that the Hamiltonians (5) or (6) yield a Schrödinger equation

$$E\psi(\boldsymbol{x}, z) = -\frac{\hbar^2}{2m}\Delta\psi(\boldsymbol{x}, z) - \frac{\hbar^2}{2\mu}\delta(z-z_0)\boldsymbol{\nabla}^2\psi(\boldsymbol{x}, z).$$

The corresponding equation for the Green's function or 2-point correlation function is

$$\begin{aligned}&\left(\frac{2m}{\hbar^2}E + \Delta + \delta(z-z_0)\frac{m}{\mu}\boldsymbol{\nabla}^2\right)\langle \boldsymbol{x}, z|G(E)|\boldsymbol{x}', z'\rangle\\ &= -\delta(\boldsymbol{x}-\boldsymbol{x}')\delta(z-z').\end{aligned} \tag{9}$$

The solution of this equation is described in the Appendix. In particular, we find the representation (see Eq. (27))

$$\begin{aligned}&\langle z|G(E,\boldsymbol{k})|z'\rangle =\\ &\frac{\hbar\Theta(\hbar^2\boldsymbol{k}^2 - 2mE)}{2\sqrt{\hbar^2\boldsymbol{k}^2 - 2mE}}\Bigg[\exp\left(-\sqrt{\hbar^2\boldsymbol{k}^2 - 2mE}\frac{|z-z'|}{\hbar}\right)\\ &-\frac{\hbar\boldsymbol{k}^2\ell}{\sqrt{\hbar^2\boldsymbol{k}^2 - 2mE} + \hbar\boldsymbol{k}^2\ell}\\ &\times\exp\left(-\sqrt{\hbar^2\boldsymbol{k}^2 - 2mE}\frac{|z-z_0| + |z'-z_0|}{\hbar}\right)\Bigg]\\ &+\mathrm{i}\frac{\hbar\Theta(2mE - \hbar^2\boldsymbol{k}^2)}{2\sqrt{2mE - \hbar^2\boldsymbol{k}^2}}\\ &\times\Bigg[\exp\left(\mathrm{i}\sqrt{2mE - \hbar^2\boldsymbol{k}^2}\frac{|z-z'|}{\hbar}\right)\\ &-\mathrm{i}\frac{\hbar\boldsymbol{k}^2\ell}{\sqrt{2mE - \hbar^2\boldsymbol{k}^2} + \mathrm{i}\hbar\boldsymbol{k}^2\ell}\\ &\times\exp\left(\mathrm{i}\sqrt{2mE - \hbar^2\boldsymbol{k}^2}\frac{|z-z_0| + |z'-z_0|}{\hbar}\right)\Bigg],\end{aligned} \tag{10}$$

where the definition $\ell \equiv m/2\mu = Lm/2m_*$ was used. The ℓ-independent terms in (10) correspond to the free Green's function $G_0(E)$ (8).

The interface at z_0 breaks translational invariance in z direction, and we have with Eq. (7)

$$\begin{aligned}\varrho(E, z) =& \frac{4m}{\pi\hbar^2}\Im\langle \boldsymbol{x}, z|G(E)|\boldsymbol{x}, z\rangle\\ =& \frac{m}{\pi^3\hbar^2}\Im\int \mathrm{d}^2\boldsymbol{k}\langle z|G(E,\boldsymbol{k})|z\rangle.\end{aligned}$$

We will use the result (10) to calculate the density of states $\varrho(E, z_0)$ in the interface. Substitution yields

$$\begin{aligned}\varrho(E, z_0) =& \frac{m}{\pi^3\hbar^2}\Im\int d^2\boldsymbol{k}\langle z_0|G(E,\boldsymbol{k})|z_0\rangle\\ =& \frac{m}{\pi^2\hbar}\Theta(E)\int_0^{\sqrt{2mE}/\hbar} dkk\frac{\sqrt{2mE - \hbar^2k^2}}{2mE - \hbar^2k^2 + \hbar^2k^4\ell^2},\end{aligned}$$

and after evaluation of the integral

$$\varrho(E,z_0) = \frac{m\Theta(E)}{2\pi^2\hbar^2\ell\sqrt{\hbar^2-8mE\ell^2}}\Theta(\hbar^2-8mE\ell^2) \times\left[2\hbar\cdot\arctan\left(\frac{\ell\sqrt{8mE}}{\hbar+\sqrt{\hbar^2-8mE\ell^2}}\right) -\frac{\pi}{2}\left(\hbar-\sqrt{\hbar^2-8mE\ell^2}\right)\right] + \frac{m\Theta(8mE\ell^2-\hbar^2)}{2\pi^2\hbar^2\ell} \times\left[\frac{\hbar}{\sqrt{8mE\ell^2-\hbar^2}}\ln\left(\frac{\ell\sqrt{8mE}-\sqrt{8mE\ell^2-\hbar^2}}{\hbar}\right)+\frac{\pi}{2}\right]. \tag{11}$$

This is a more complicated result than the density (1) for $d = 2$ or $d = 3$. However, it reduces to either the two-dimensional or three-dimensional density of states in the appropriate limits, see Fig. 1. For large energies, i.e. if the states only probe length scales smaller than the transition length scale ℓ, we find the two-dimensional density of states properly rescaled by a dimensional factor to reflect that it is a density of states per three-dimensional volume,

$$8mE\ell^2 \gg \hbar^2: \quad \varrho(E,z_0)\to\Theta(E)\frac{m}{4\pi\hbar^2\ell}=\frac{1}{4\ell}\varrho_{(d=2)}(E). \tag{12}$$

For small energies, i.e. if the states probe length scales larger than ℓ, we find the three-dimensional density of states

$$8mE\ell^2 \ll \hbar^2: \quad \varrho(E,z_0)\to\Theta(E)\frac{\sqrt{2m^3}}{\pi^2\hbar^3}\sqrt{E}=\varrho_{(d=3)}(E). \tag{13}$$

This limiting behavior for interpolation between two and three dimensions is consistent with what is also observed for the zero-energy Green's function in the interface, see equations (21–22) below.

Equation (11) also implies interpolating behavior for the relation between electron density and Fermi energy on the interface. The full relation is

$$n(z_0) = \frac{\sqrt{mE_F}}{\sqrt{8}\pi^2\hbar\ell^2}-\frac{1}{16\pi\ell^3}+\frac{\Theta(\hbar^2-8mE_F\ell^2)}{8\pi^2\hbar^2\ell^3} \times\left[\frac{\pi}{2}\left(4mE_F\ell^2+\hbar\sqrt{\hbar^2-8mE_F\ell^2}\right) -2\hbar\sqrt{\hbar^2-8mE_F\ell^2}\cdot\arctan\left(\frac{\sqrt{8mE_F}\ell}{\hbar+\sqrt{\hbar^2-8mE_F\ell^2}}\right)\right] + \frac{\Theta(8mE_F\ell^2-\hbar^2)}{8\pi^2\hbar\ell^3} \times\left[\sqrt{8mE_F\ell^2-\hbar^2}\ln\left(\frac{\sqrt{8mE_F}\ell-\sqrt{8mE_F\ell^2-\hbar^2}}{\hbar}\right) +\frac{2\pi mE_F\ell^2}{\hbar}\right].$$

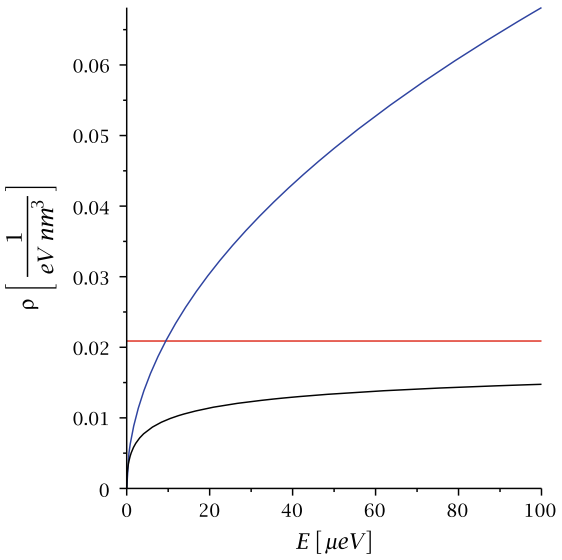

Fig. 1 The *red line* is the two-dimensional limit (12). The *blue line* is the three-dimensional density of states. The it black line is the inter-dimensional density of states (11) for $\ell = 50$ nm

This approximates two-dimensional behavior for $mE_F\ell^2 \gg \hbar^2$,

$$n(z_0)\simeq\frac{mE_F}{4\pi\hbar^2\ell}=\frac{1}{4\ell}n_{(d=2)},$$

and three-dimensional behavior for $mE_F\ell^2 \ll \hbar^2$,

$$n(z_0)\simeq\frac{\sqrt{2mE_F}^3}{3\pi^2\hbar^3}=n_{(d=3)}.$$

It is intuitively understandable that the presence of a layer reduces the available density of states for given energy, or equivalently increases the Fermi energy for a given density of electrons. The presence of a layer generically implies boundary or matching conditions which reduce the number of available states at a given energy.

A condition for relevance of the inter-dimensional behavior is a large transition scale compared to the layer thickness, $\ell \gg L$, see also Fig. 2. In terms of effective particle mass, this means

$$m \gg m_*, \tag{14}$$

i.e. the energy band in the interface should be more strongly curved than in the bulk matrix for the transition to two-dimensional behavior to be observable.

Electric Fields in the Presence of High-Permittivity Thin Films or Interfaces

The zero-energy Green's function $G(r) \equiv \langle\vec{x}|G(E=0)|\vec{x}'\rangle|_{r=|\vec{x}-\vec{x}'|}$ determines electrostatic and exchange

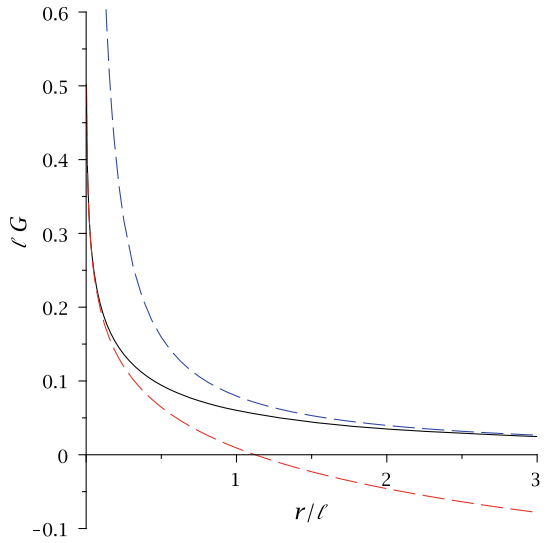

Fig. 2 *The upper dotted (blue) line* is the three-dimensional Green's function $(4\pi r)^{-1}$ in units of ℓ^{-1}, the continuous line is the Green's function (19) in units of ℓ^{-1}, and the *lower dotted (red) line* is the two-dimensional logarithmic Green's function $\ell \cdot G = -(\gamma + \ln(r/2\ell))/(4\pi)$

interactions through the electrostatic potential $\Phi(r) = qG(r)/\epsilon$. Here, q is an electric charge in a dielectric material of permittivity ϵ. The zero-energy Green's function in d spatial dimensions is given by

$$G(r) = \begin{cases} -r/2, & d = 1, \\ -(2\pi)^{-1}\ln(r/a), & d = 2, \\ \Gamma\left(\frac{d-2}{2}\right)\left(4\sqrt{\pi}^{d} r^{d-2}\right)^{-1}, & d \geq 3. \end{cases} \tag{15}$$

We cannot infer from the previous section that the zero energy limit of the inter-dimensional Green's function calculated there also yields a dimensionally hybrid potential, because we were dealing with solutions of Schrödinger's equation instead of the Gauss law. However, we can rederive the zero energy limit of that Green's function from the Gauss law for electromagnetic fields in the presence of a high-permittivity interface.

Suppose we have charge carriers of charge q and mass m in the presence of an interface with permittivity ϵ_* and permeability μ_*, We continue to denote vectors parallel to the interface in bold face notation, $\vec{x} = \{\boldsymbol{x}, z\}$, $\vec{\nabla} = \{\boldsymbol{\nabla}, \partial_z\}, \vec{A} = \{\boldsymbol{A}, A_z\}$, etc.

If the photon wavelengths and incidence angles satisfy the condition $\lambda \gg 2\pi L|\cos\vartheta|$, we can approximate the system with an action

$$S = L\int \mathrm{d}^2\boldsymbol{x}\left[\frac{\epsilon_*}{2}\vec{E}^2 - \frac{1}{2\mu_*}\vec{B}^2\right]_{z=z_0} + \int \mathrm{d}^3\vec{x}\left[\frac{\mathrm{i}\hbar}{2}\left(\psi^+\cdot\frac{\partial}{\partial t}\psi - \frac{\partial}{\partial t}\psi^+\cdot\psi\right) - q\psi^+\Phi\psi + \frac{q\hbar}{2m}\psi^+\vec{\sigma}\cdot\vec{B}\psi + \frac{1}{2m}\left(\mathrm{i}\hbar\vec{\nabla}\psi^+ - q\psi^+\vec{A}\right)\cdot\left(\mathrm{i}\hbar\vec{\nabla}\psi + q\vec{A}\psi\right) + \frac{\epsilon}{2}\vec{E}^2 - \frac{1}{2\mu}\vec{B}^2\right].$$

Variation with respect to the electrostatic potential, $\delta S/\delta\Phi = 0$, yields the Gauss law in the form

$$\epsilon\vec{\nabla}\cdot\vec{E} + L\epsilon_*\delta(z - z_0)\boldsymbol{\nabla}\cdot\boldsymbol{E} = q\psi^+\psi \tag{16}$$

and the continuity condition $E_z(z_0 - 0) = E_z(z_0 + 0)$.

We solve Eq. (16) in Coulomb gauge,

$$\Phi(\vec{x}, t) = \frac{q}{\epsilon}\int \mathrm{d}^3\vec{x}' G(\vec{x}, \vec{x}')\psi^+(\vec{x}', t)\psi(\vec{x}', t) \tag{17}$$

where the Green's function has to satisfy

$$\Delta G(\vec{x}, \vec{x}') + L\frac{\epsilon_*}{\epsilon}\delta(z - z_0)\boldsymbol{\nabla}^2 G(\vec{x}, \vec{x}') = -\delta(\vec{x} - \vec{x}'). \tag{18}$$

This equation is the zero energy limit of Eq. (9) with the substitution

$$\frac{m}{\mu} \equiv L\frac{m}{m_*} \to L\frac{\epsilon_*}{\epsilon}.$$

We can therefore read off the solution from the results of the previous section with $E = 0$ and now $\ell \equiv L\epsilon_*/2\epsilon$.

Equation (10) yields in particular

$$\langle z|G(\boldsymbol{k})|z'\rangle = \frac{1}{2\mathrm{k}}\left(\exp(-\mathrm{k}|z - z'|) - \frac{\mathrm{k}\ell\exp(-\mathrm{k}|z - z_0| - \mathrm{k}|z' - z_0|)}{1 + \mathrm{k}\ell}\right)$$

with $\mathrm{k} \equiv |\boldsymbol{k}|$. Fourier transformation yields

$$\begin{aligned}\langle z|G(\boldsymbol{x})|z'\rangle &= \int_0^\infty d\mathrm{k}\int_0^{2\pi} d\varphi\frac{\exp(\mathrm{ik}|\boldsymbol{x}|\cos\varphi)}{8\pi^2} \\ &\quad\times\left(\exp(-\mathrm{k}|z - z'|)\right. \\ &\quad\left.-\frac{\mathrm{k}\ell\exp(-\mathrm{k}|z - z_0| - \mathrm{k}|z' - z_0|)}{1 + \mathrm{k}\ell}\right) \\ &= \int_0^\infty\frac{d\mathrm{k}}{4\pi}\left(\exp(-\mathrm{k}|z - z'|)\right. \\ &\quad\left.-\frac{\mathrm{k}\ell\exp(-\mathrm{k}|z - z_0| - \mathrm{k}|z' - z_0|)}{1 + \mathrm{k}\ell}\right)J_0(\mathrm{k}|\boldsymbol{x}|).\end{aligned} \tag{19}$$

The zero-energy Green's function in the interface is given in terms of a Struve function and a Neumann function[1],

[1] Our notations for special functions follow the conventions of Abramowitz and Stegun [16].

$$G(r) = \langle z_0|G(r = |\boldsymbol{x} - \boldsymbol{x}'|)|z_0\rangle = \int_0^\infty \frac{\mathrm{d}k}{4\pi}\frac{J_0(kr)}{1 + k\ell} = \frac{1}{8\ell}\left[\boldsymbol{H}_0\left(\frac{r}{\ell}\right) - Y_0\left(\frac{r}{\ell}\right)\right]. \quad (20)$$

This yields logarithmic behavior of interaction potentials at small distances $r \ll \ell$ and $1/r$ behavior for large separation $r \gg \ell$ of charges in high-permittivity thin films,

$$r \ll \ell: \quad G(r) = \frac{1}{4\pi\ell}\left[-\gamma - \ln\left(\frac{r}{2\ell}\right) + \frac{r}{\ell} + \mathcal{O}\left(\frac{r^2}{\ell^2}\right)\right], \quad (21)$$

$$r \gg \ell: \quad G(r) = \frac{1}{4\pi r}\left[1 - \frac{\ell^2}{r^2} + \mathcal{O}\left(\frac{\ell^4}{r^4}\right)\right], \quad (22)$$

see also Fig. 2.

For the comparison with image charges, we set $z_0 = 0$ and recall that the solution for the potential of a charge q at $\boldsymbol{x} = 0$, $z = 0$ proceeds through the *ansatz*

$$|z| \le L/2: \ \Phi = \frac{1}{4\pi\epsilon_*}\left[\frac{q}{\sqrt{r^2+z^2}} + \sum_{n=1}^{\infty} q_n\left(\frac{1}{\sqrt{r^2+(z-nL)^2}} + \frac{1}{\sqrt{r^2+(z+nL)^2}}\right)\right] = \sum_{n=-\infty}^{\infty}\frac{q_{|n|}}{4\pi\epsilon_*\sqrt{r^2+(z-nL)^2}},$$

$$z > L/2: \ \Phi = \frac{1}{4\pi\epsilon}\left(\frac{Q}{\sqrt{r^2+z^2}} + \sum_{n=1}^{\infty}\frac{Q_n}{\sqrt{r^2+(z+nL)^2}}\right) = \sum_{n=0}^{\infty}\frac{Q_n}{4\pi\epsilon\sqrt{r^2+(z+nL)^2}},$$

and symmetric continuation to $z < -L/2$.

This yields electric fields

$$|z| \le L/2: \quad E_r = \sum_{n=-\infty}^{\infty}\frac{q_{|n|}r}{4\pi\epsilon_*\sqrt{r^2+(z-nL)^2}^3}, \quad E_z = \sum_{n=-\infty}^{\infty}\frac{q_{|n|}(z-nL)}{4\pi\epsilon_*\sqrt{r^2+(z-nL)^2}^3},$$

$$z > L/2: \quad E_r = \sum_{n=0}^{\infty}\frac{Q_n r}{4\pi\epsilon\sqrt{r^2+(z+nL)^2}^3}, \quad E_z = \sum_{n=0}^{\infty}\frac{Q_n(z+nL)}{4\pi\epsilon\sqrt{r^2+(z+nL)^2}^3},$$

and the junction conditions at $z = L/2$ yield for $n \ge 0$ from the continuity of E_r,

$$\frac{q_n + q_{n+1}}{\epsilon_*} = \frac{Q_n}{\epsilon},$$

and from the continuity of D_z,

$$q_n - q_{n+1} = Q_n.$$

These conditions can be solved through

$$q_n = \left(\frac{\epsilon_* - \epsilon}{\epsilon_* + \epsilon}\right)^n q, \quad Q_n = \frac{2\epsilon}{\epsilon_* + \epsilon}\left(\frac{\epsilon_* - \epsilon}{\epsilon_* + \epsilon}\right)^n q,$$

$$|z| \le L/2: \quad \Phi = \frac{q}{4\pi\epsilon_*}\sum_{n=-\infty}^{\infty}\left(\frac{\epsilon_* - \epsilon}{\epsilon_* + \epsilon}\right)^{|n|}\frac{1}{\sqrt{r^2+(z-nL)^2}},$$

$$z > L/2: \quad \Phi = \frac{q}{2\pi(\epsilon_* + \epsilon)}\sum_{n=0}^{\infty}\left(\frac{\epsilon_* - \epsilon}{\epsilon_* + \epsilon}\right)^{n}\frac{1}{\sqrt{r^2+(z+nL)^2}}.$$

In particular, the potential at $z = 0$ is

$$\Phi(r) = \frac{q}{4\pi\epsilon_* r} + \frac{q}{2\pi\epsilon_*}\sum_{n=1}^{\infty}\left(\frac{\epsilon_* - \epsilon}{\epsilon_* + \epsilon}\right)^{n}\frac{1}{\sqrt{r^2+n^2L^2}}. \quad (23)$$

We have

$$\sum_{n=1}^{\infty}\left(\frac{\epsilon_* - \epsilon}{\epsilon_* + \epsilon}\right)^n = \frac{\epsilon_* - \epsilon}{2\epsilon}$$

and therefore for $\epsilon_* > \epsilon$

$$\frac{q}{4\pi\epsilon_* r} < \Phi(r) \le \Phi(r)\Big|_{a=0} = \frac{q}{4\pi\epsilon r}.$$

The solution from image charges is in very good agreement with the analytic model for distances $r \gtrsim L/2$, where both the image charge solution and the analytic model show strong deviations from the bulk r^{-1} behavior. This is illustrated in Fig. 3 by plotting the reduced electrostatic potential for a charge q, $\epsilon L\Phi(r)/q = LG(r)$ in the interface.

It is also instructive to plot the relative deviation $(\Phi_{image} - \Phi_{hybrid})/\Phi_{image}$ between the dimensionally hybrid potential $\Phi_{hybrid}(r) = qG(r)/\epsilon$ which follows from (20) and the potential Φ_{image} (23) from image charges.

Figure 4 shows that for $r \gtrsim L/2$, the dimensionally hybrid model is a very good approximation to the potential from image charges with accuracy better than 10^{-2} if $\epsilon_*/\epsilon = 100$. For $\epsilon_*/\epsilon = 10$, the accuracy is still better than 4×10^{-2}.

Summary

An analysis of models for particles in the presence of a low effective mass interface, and for electromagnetic fields in the presence of a high-permittivity thin film, yields dimensionally hybrid densities of states (11) and electrostatic potentials (17,20) which interpolate between two-

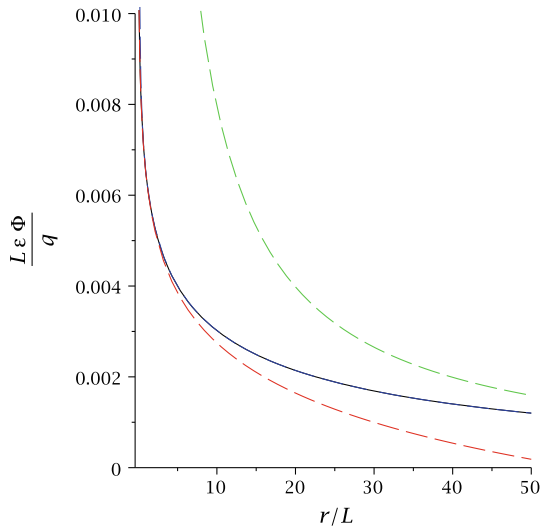

Fig. 3 Different reduced electrostatic potentials are plotted for $\epsilon_*/\epsilon = 100$. The *upper dotted (green) line* is the three-dimensional reduced potential $L/(4\pi r)$. The *central dotted (blue) line* is the reduced potential following from the image charge solution (22). The *solid (black) line* is the potential from the analytic model (19). The *lower dotted (red) line* is the reduced logarithmic potential. The reduced potentials from our analytic model and from image charges are indistinguishable for $r > rsimL/2$, see also Fig. 4

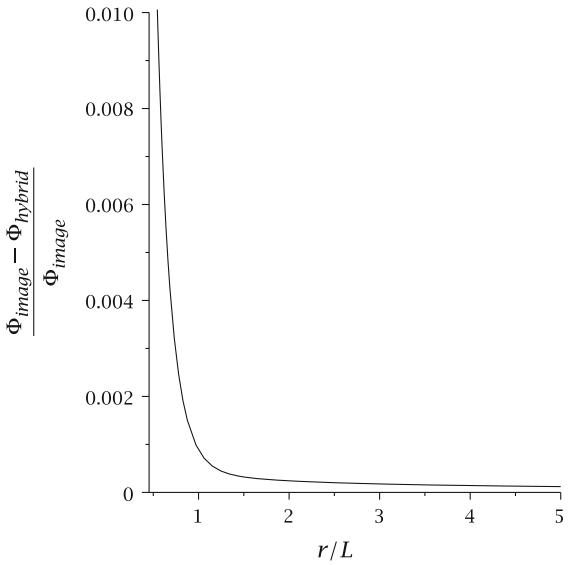

Fig. 4 The relative deviation $(\Phi_{image} - \Phi_{hybrid})/\Phi_{image}$ between the dimensionally hybrid potential from (19) and the potential (22) from image charges for $\epsilon_*/\epsilon = 100$

dimensional behavior and three-dimensional behavior. The analytic model for the electromagnetic fields is in very good agreement with the infinite series solution already for small distance scales $r \gtrsim L/2$, where the potential strongly deviates from the standard bulk r^{-1} potential. At distance scales smaller than $L/2$, r^{-1}, behavior seems to dominate again for the electrostatic potential, in agreement with expectations that for distances which are small compared to the lateral extension of a dielectric slab, bulk behavior should be restored. However, note that neither the inter-dimensional analytic model nor the solution from image charges is trustworthy for very small distances, because both models rely on a continuum approximation through the use of effective permittivities, but the continuum approximation should break down at sub-nanometer scales.

The most important finding is that interfaces and thin films of width L should exhibit transitions between two-dimensional and three-dimensional distance laws for physical quantities at length scales of order $Lm/2m_*$ or $L\epsilon_*/2\epsilon$, respectively. Interfaces with strong band curvature or high permittivity should provide good samples for experimental study of the transition between two-dimensional and three-dimensional behavior.

Acknowledgements This research was supported by NSERC Canada.

Appendix: Solution of Eq. (9)

Substitution of the Fourier transform

$$\langle \boldsymbol{x}, z|G(E)|\boldsymbol{x}', z'\rangle = \frac{1}{4\pi^2}\int \mathrm{d}^2\boldsymbol{k}\int \mathrm{d}^2\boldsymbol{k}'\langle \boldsymbol{k}, z|G(E)|\boldsymbol{k}', z'\rangle \exp[\mathrm{i}(\boldsymbol{k}\cdot\boldsymbol{x} - \boldsymbol{k}'\cdot\boldsymbol{x}')]$$

into Eq. (9) yields

$$\left(\frac{2m}{\hbar^2}E - \boldsymbol{k}^2 + \partial_z^2\right)\langle \boldsymbol{k}, z|G(E)|\boldsymbol{k}', z'\rangle - \frac{m}{\mu}\boldsymbol{k}^2\delta(z-z_0)\langle \boldsymbol{k}, z|G(E)|\boldsymbol{k}', z'\rangle = -\delta(\boldsymbol{k}-\boldsymbol{k}')\delta(z-z'). \quad (24)$$

This yields with (7) the condition

$$\left(\frac{2m}{\hbar^2}E - \boldsymbol{k}^2 + \partial_z^2\right)\langle z|G(E,\boldsymbol{k})|z'\rangle - \frac{m}{\mu}\boldsymbol{k}^2\delta(z-z_0)\langle z|G(E,\boldsymbol{k})|z'\rangle = -\delta(z-z').$$

Fourier transformation with respect to z yields

$$\left(\frac{2m}{\hbar^2}E - \boldsymbol{k}^2 - k_\perp^2\right)\langle k_\perp|G(E,\boldsymbol{k})|z'\rangle - \frac{m}{2\pi\mu}\boldsymbol{k}^2\int \mathrm{d}\kappa_\perp \exp[\mathrm{i}(\kappa_\perp - k_\perp)z_0]\langle \kappa_\perp|G(E,\boldsymbol{k})|z'\rangle = -\frac{1}{\sqrt{2\pi}}\exp(-\mathrm{i}k_\perp z'). \quad (25)$$

This result implies that $\langle k_\perp|G(E,\boldsymbol{k})|z'\rangle$ has the form

$$\exp(\mathrm{i}k_\perp z_0)\langle k_\perp|G(E,\boldsymbol{k})|z'\rangle = \frac{(\exp[\mathrm{i}k_\perp(z_0-z')]/\sqrt{2\pi})+f(E,\boldsymbol{k},z')}{k_\perp^2+\boldsymbol{k}^2-(2mE/\hbar^2)}$$

with the yet to be determined function $f(E,\boldsymbol{k},z')$ satisfying

$$f(E,\boldsymbol{k},z') + \frac{m}{2\pi\mu}\boldsymbol{k}^2\int \mathrm{d}\kappa_\perp \frac{(\exp[\mathrm{i}\kappa_\perp(z_0-z')]/\sqrt{2\pi})+f(E,\boldsymbol{k},z')}{\kappa_\perp^2+\boldsymbol{k}^2-(2mE/\hbar^2)} = 0.$$

For the treatment of the integrals, we should be consistent with the calculation of the free retarded Green's function (8),

$$\int\frac{\mathrm{d}\kappa_\perp}{2\pi}\frac{\exp(\mathrm{i}\kappa_\perp z)}{\kappa_\perp^2+\boldsymbol{k}^2-(2mE/\hbar^2)-\mathrm{i}\epsilon} = \frac{\hbar}{2}\Theta(\hbar^2\boldsymbol{k}^2-2mE)\frac{\exp\left(-\sqrt{\hbar^2\boldsymbol{k}^2-2mE}|z|/\hbar\right)}{\sqrt{\hbar^2\boldsymbol{k}^2-2mE}} + \mathrm{i}\frac{\hbar}{2}\Theta(2mE-\hbar^2\boldsymbol{k}^2)\frac{\exp\left(\mathrm{i}\sqrt{2mE-\hbar^2\boldsymbol{k}^2}|z|/\hbar\right)}{\sqrt{2mE-\hbar^2\boldsymbol{k}^2}}.$$

This yields

$$\left[1+\frac{m\hbar}{2\mu}\boldsymbol{k}^2\left(\frac{\Theta(\hbar^2\boldsymbol{k}^2-2mE)}{\sqrt{\hbar^2\boldsymbol{k}^2-2mE}}+\mathrm{i}\frac{\Theta(2mE-\hbar^2\boldsymbol{k}^2)}{\sqrt{2mE-\hbar^2\boldsymbol{k}^2}}\right)\right]\times f(E,\boldsymbol{k},z') = -\frac{m\hbar}{2\mu\sqrt{2\pi}}\boldsymbol{k}^2\left[\frac{\Theta(\hbar^2\boldsymbol{k}^2-2mE)}{\sqrt{\hbar^2\boldsymbol{k}^2-2mE}}\times\exp\left(-\sqrt{\hbar^2\boldsymbol{k}^2-2mE}\frac{|z'-z_0|}{\hbar}\right)+\mathrm{i}\frac{\Theta(2mE-\hbar^2\boldsymbol{k}^2)}{\sqrt{2mE-\hbar^2\boldsymbol{k}^2}}\exp\left(\mathrm{i}\sqrt{2mE-\hbar^2\boldsymbol{k}^2}\frac{|z'-z_0|}{\hbar}\right)\right],$$

and therefore

$$\begin{aligned}\langle k_\perp|G(E,\boldsymbol{k})|z'\rangle = {}& \frac{1}{\sqrt{2\pi}}\frac{1}{k_\perp^2+\boldsymbol{k}^2-(2mE/\hbar^2)-\mathrm{i}\epsilon}\\ &\times\Big[\exp(-\mathrm{i}k_\perp z')\\ &-\frac{\hbar\boldsymbol{k}^2\ell\Theta(\hbar^2\boldsymbol{k}^2-2mE)}{\sqrt{\hbar^2\boldsymbol{k}^2-2mE}+\hbar\boldsymbol{k}^2\ell}\\ &\times\exp\left(-\mathrm{i}k_\perp z_0-\sqrt{\hbar^2\boldsymbol{k}^2-2mE}\frac{|z'-z_0|}{\hbar}\right)\\ &-\mathrm{i}\frac{\hbar\boldsymbol{k}^2\ell\Theta(2mE-\hbar^2\boldsymbol{k}^2)}{\sqrt{2mE-\hbar^2\boldsymbol{k}^2}+\mathrm{i}\hbar\boldsymbol{k}^2\ell}\\ &\times\exp\left(-\mathrm{i}k_\perp z_0+\mathrm{i}\sqrt{2mE-\hbar^2\boldsymbol{k}^2}\frac{|z'-z_0|}{\hbar}\right)\Big],\end{aligned} \tag{26}$$

where the definition $\ell\equiv m/2\mu = Lm/2m_*$ was used. Fourier transformation of Eq. (26) with respect to $k_\perp$ yields finally

$$\begin{aligned}\langle z|G(E,\boldsymbol{k})|z'\rangle = {}& \frac{\hbar\Theta(\hbar^2\boldsymbol{k}^2-2mE)}{2\sqrt{\hbar^2\boldsymbol{k}^2-2mE}}\Big[\exp\left(-\sqrt{\hbar^2\boldsymbol{k}^2-2mE}\frac{|z-z'|}{\hbar}\right)\\ &-\frac{\hbar\boldsymbol{k}^2\ell}{\sqrt{\hbar^2\boldsymbol{k}^2-2mE}+\hbar\boldsymbol{k}^2\ell}\\ &\times\exp\left(-\sqrt{\hbar^2\boldsymbol{k}^2-2mE}\frac{|z-z_0|+|z'-z_0|}{\hbar}\right)\Big]\\ &+\mathrm{i}\frac{\hbar\Theta(2mE-\hbar^2\boldsymbol{k}^2)}{2\sqrt{2mE-\hbar^2\boldsymbol{k}^2}}\Big[\exp\left(\mathrm{i}\sqrt{2mE-\hbar^2\boldsymbol{k}^2}\frac{|z-z'|}{\hbar}\right)\\ &-\mathrm{i}\frac{\hbar\boldsymbol{k}^2\ell}{\sqrt{2mE-\hbar^2\boldsymbol{k}^2}+\mathrm{i}\hbar\boldsymbol{k}^2\ell}\\ &\times\exp\left(\mathrm{i}\sqrt{2mE-\hbar^2\boldsymbol{k}^2}\frac{|z-z_0|+|z'-z_0|}{\hbar}\right)\Big].\end{aligned} \tag{27}$$

The Green's function with only k space variables

$$\langle\boldsymbol{k},k_\perp|G(E)|\boldsymbol{k}',k'_\perp\rangle = \langle k_\perp|G(E;\boldsymbol{k})|k'_\perp\rangle\delta(\boldsymbol{k}-\boldsymbol{k}')$$

is found from the Fourier transform of Eq. (25),

$$\left(\boldsymbol{k}^2+k_\perp^2-\frac{2m}{\hbar^2}E\right)\langle k_\perp|G(E,\boldsymbol{k})|k'_\perp\rangle+\frac{\ell}{\pi}\boldsymbol{k}^2\int\mathrm{d}\kappa_\perp\exp[\mathrm{i}(\kappa_\perp-k_\perp)z_0]\langle\kappa_\perp|G(E,\boldsymbol{k})|k'_\perp\rangle = \delta(k_\perp-k'_\perp)$$

and the ensuing equations

$$\exp(\mathrm{i}k_\perp z_0)\langle k_\perp|G(E,\boldsymbol{k})|k'_\perp\rangle = \frac{\exp(\mathrm{i}k_\perp z_0)\delta(k_\perp-k'_\perp)+f(E,\boldsymbol{k},k'_\perp)}{k_\perp^2+\boldsymbol{k}^2-(2mE/\hbar^2)},$$

$$f(E,\boldsymbol{k},k'_\perp)+\frac{\boldsymbol{k}^2\ell}{\pi}f(E,\boldsymbol{k},k'_\perp)\int\frac{\mathrm{d}\kappa_\perp}{\kappa_\perp^2+\boldsymbol{k}^2-(2mE/\hbar^2)} = -\frac{\boldsymbol{k}^2\ell}{\pi}\frac{\exp(\mathrm{i}k'_\perp z_0)}{k_\perp'^2+\boldsymbol{k}^2-(2mE/\hbar^2)}.$$

This yields

$$\begin{aligned}\langle k_\perp|G(E,\boldsymbol{k})|k'_\perp\rangle = {}& \frac{1}{k_\perp^2+\boldsymbol{k}^2-(2mE/\hbar^2)-\mathrm{i}\epsilon}\Big[\delta(k_\perp-k'_\perp)\\ &-\frac{\boldsymbol{k}^2\ell}{\pi}\frac{\exp[\mathrm{i}(k'_\perp-k_\perp)z_0]}{k_\perp'^2+\boldsymbol{k}^2-(2mE/\hbar^2)-\mathrm{i}\epsilon}\\ &\times\left(\frac{\sqrt{\hbar^2\boldsymbol{k}^2-2mE}\Theta(\hbar^2\boldsymbol{k}^2-2mE)}{\sqrt{\hbar^2\boldsymbol{k}^2-2mE}+\hbar\boldsymbol{k}^2\ell}+\frac{\sqrt{2mE-\hbar^2\boldsymbol{k}^2}\Theta(2mE-\hbar^2\boldsymbol{k}^2)}{\sqrt{2mE-\hbar^2\boldsymbol{k}^2}+\mathrm{i}\hbar\boldsymbol{k}^2\ell}\right)\Big].\end{aligned}$$

It is easily verified that Fourier transformation yields again the result (26).

References

1. R. Dick, Int. J. Theor. Phys. **42**, 569 (2003)
2. R. Dick, Nanoscale Res. Lett. **3**, 140 (2008)
3. R. Dick, Phys. E **40**, 524 (2008)
4. R. Dick, Phys. E **40**, 2973 (2008)
5. Y.A. Bychkov, E.I. Rashba, JETP Lett. **39**, 78 (1984)
6. Y.A. Bychkov, E.I. Rashba, J. Phys. C **17**, 6039 (1984)
7. E. Cappelluti, C. Grimaldi, F. Marsiglio, Phys. Rev. Lett. **98**, 167002 (2007)
8. E. Cappelluti, C. Grimaldi, F. Marsiglio, Phys. Rev. B **76**, 085334 (2007)
9. B. Srisongmuang, P. Pairor, M. Berciu, Phys. Rev. B **78**, 155317 (2008)
10. P. Vasilopoulos, X.F. Wang, Phys. E **40**, 1729 (2008)
11. S.-S. Li, J.-B. Xia, Nanoscale Res. Lett. **4**, 178 (2009)
12. G.W. Semenoff, Phys. Rev. Lett. **53**, 2449 (1984)
13. V. Apalkov, X.F. Wang, T. Chakraborty, Int. J. Mod. Phys. B **21**, 1165 (2007)
14. L. Covaci, M. Berciu, Phys. Rev. Lett. **100**, 256405 (2008)
15. T. Li, Z. Zhang, Nanoscale Res. Lett. **5**, 169 (2010)
16. M. Abramowitz, I.A. Stegun (eds.), *Handbook of Mathematical Functions, 9th printing*, (Dover Publications, New York, 1970)